# Comparison of low-energy $\beta$ radiation effects in polyethylene and cellulose

Jussi Polvi, Kai Nordlund

*Department of Physics, P. O. Box 43, FIN-00014 University of Helsinki, Finland*

**Abstract**

Using molecular dynamics simulations, we have compared the low-energy $\beta$ radiation effects in high density polyethylene and cellulose. We determined the threshold energy for creating defects as a function of the incident angle, for a carbon atom in polyethylene chain, and for one of the carbon atoms in cellulose chain. Our analysis shows that the damage threshold energy is in the both cases strongly dependent on the initial recoil direction and on average slightly higher for the carbon atoms in the polyethylene chain than for the target carbon atom in cellulose chain.
**Keywords:** molecular dynamics, polyethylene, cellulose, irradiation, damage threshold energy

## 1. Introduction

Polymeric materials such as plastics and rubber are subject to irradiation in nature due to ultra-violet light from the sun, and this is in fact a common reason for degradation of their properties. Irradiation has also been deliberately used to process and modify polymeric materials since the 1960s [1]. The practical applications include cross-linking plastic materials, sterilizing medical equipment, preserving food products and making hydrogels for medical applications [2, 3].

In this article we examine irradiation-induced defects in two polymeric materials, high density polyethylene (HDPE) and cellulose I$\beta$, using molecular dynamics (MD) simulations. Polyethylene (PE) is structurally and conceptually the simplest of the organic polymers and cellulose is one of the basic biopolymers and structural components of wood and plant fibers [4].

A considerable number of experimental studies relating to radiation chemistry and physics of polyethylene [5, 6, 7, 8, 9] has been published but only few computational studies are available [10]. Some recent experimental studies on the irradiation of cellulose are available [11, 12, 13, 14] but none where MD-simulations would have been utilized. In a recent article by us [15] the formation of radiation defects in HDPE and cellulose was studied using MD simulations. In this work we expand and improve the previous analysis and study the threshold energy for damage production in more detail.

*Email address:* jussi.polvi@helsinki.fi (Jussi Polvi)

## 2. Methods

Irradiation effects in HDPE and cellulose were studied using molecular dynamics simulations [16]. The HDPE simulations were carried out with the PARCAS code [17]. The inter-atomic interactions were modeled with the reactive hydrocarbon potential AIREBO [18, 19], which is based on the reactive potential model REBO, developed by Brenner [20]. For cellulose simulations involving oxygen, we used the REBO potential for C, H and O interactions by Ni et al. [21] that was recently improved and updated by Kemper and Sinnott [22]. These simulations were carried out using a MD code written by Travis Kemper, the same code that was used in [22].

The simulation method used to study the irradiation process inside a bulk HDPE and cellulose is described in the Methods section of Ref. [15].

Two types of simulations were carried in this work: *damage threshold simulations* and *recoil event simulations*.

First, to compare the threshold for damage production in HDPE and cellulose, we gave the target carbon atom, either in HDPE or cellulose, a recoil energy in a random direction. Using a binary search algorithm, we tuned the energy until we had pinpointed the threshold energy for creating damage in the sample by 0.5 eV precision. This process was then repeated 500 times for both targets to get a good coverage of all incident angles.

The definition for 'damage', used in our damage threshold simulations, is that at least one bond in the

target sample is broken as a consequence of the recoil event. This means that the target atom and its bonds may be unaffected if the broken bond is a secondary effect. The simulation time used in these simulations was 3 ps.

In the recoil event simulations, 100 simulations were carried out per recoil energies 50 and 100 eV. Each HDPE simulation was run for 10 ps to give the system some time to relax after the initial recoil. Because of the more complex structure of the cellulose molecule, we used longer simulation time of 20 ps for cellulose simulations. In 50 HDPE simulations a random hydrogen atom was chosen as a recoil atom, and in another 50 simulations, a random carbon atom. The single impact simulation process identical to the one used in in Ref. [15]. For cellulose, we use the data from single impact simulations done in Ref. [15].

## 3. Results and discussion

In the damage threshold simulations, the size of the HDPE simulation box was $x$=2.9 nm, $y$=2.5 nm and $z$=2.6 nm, containing 2400 atoms. For the cellulose, a simulation box of size $x$=2.3 nm, $y$=2.5 nm and $z$=3.1 nm, was used, containing 2268 atoms. In both materials the polymer chains were oriented along the $z$-axis.

In the recoil event simulations, the size of the HDPE simulation box was $x$=2.9 nm, $y$=3.6 nm and $z$=4.1 nm with 5376 atoms, and the size of cellulose simulation box was $x$=3.3 nm, $y$=3.5 nm and $z$=3.1 nm with 4032 atoms. Irradiation of the HDPE system with 10 eV of energy corresponds to a 38 kGy dose of ionizing radiation and for the cellulose system the same irradiation energy corresponds to a dose of 31 kGy.

### *3.1. Damage threshold simulations*

In the the damage threshold simulations we we modelled the threshold energy for damage production for a single C atom in PE and cellulose, highlighted green in Fig. 1. From the D-glucose unit of cellulose we chose the target carbon as shown in the RHS of Fig. 1 since it has on the other hand most similar surroundings compared to the C target in PE, and on the other hand it differs by having an asymmetrical C and O bonds. Both polymer chains are oriented along the $z$-axis, and in the following energy maps, the 'up' or 'north' direction is same as 'up' in the Fig. 1.

Based on our simulations the average energy needed to create damage in the PE sample 19.9 eV for C recoils. This is in good agreement with TEM experiments, according to which the electron energy needed to induce

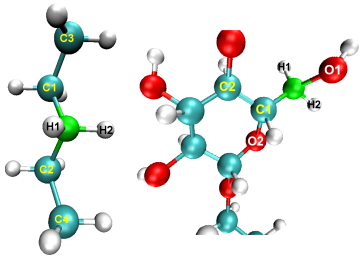


Figure 1: A visualization of the recoil atoms for damage threshold simulations. On the left is shown the recoiling carbon atom (green) in polyethylene chain and on the right the recoiling carbon atom (green) on cellulose chain. The numbers drawn on the atoms correspond to the numbers on energy landscape images.

defects in polyethylene is about 100 keV [23]. This corresponds to a maximal energy transfer of 20 eV to a carbon atom.

For the carbon recoil in cellulose the average damage threshold energy was 16.9 eV. Higher threshold energy for the C atom in PE is to be expected, since the target atom is a part of the polymer chain and if a bond with one it's C neighbours is broken, the chain holds the dangling bond in the close proximity of the recoil atom thus making the reformation of the bond easy. If the carbon atom in the cellulose target loses it's carbon or oxygen neighbours, a radical OH or $CH_2OH$ is created, and the radical likely moves further away from the recoil site after the recoil event. This process is demonstrated in the image sequence of Fig. 2.

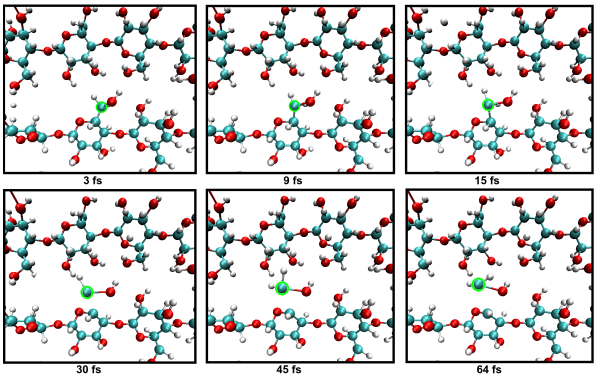


Figure 2: Image sequence showing the creation of radical $CH_2OH$ as a consequence of 30 eV carbon recoil in the cellulose sample. The recoiling atom is highlighted with a green halo.

In Fig. 3 we have the energy landscapes of the damage threshold energy for a carbon atom in PE and cellulose chains. Both damage threshold energy maps are based on 500 recoil events with a random initial recoil direction. Note that as spherical maps stretched to pla-

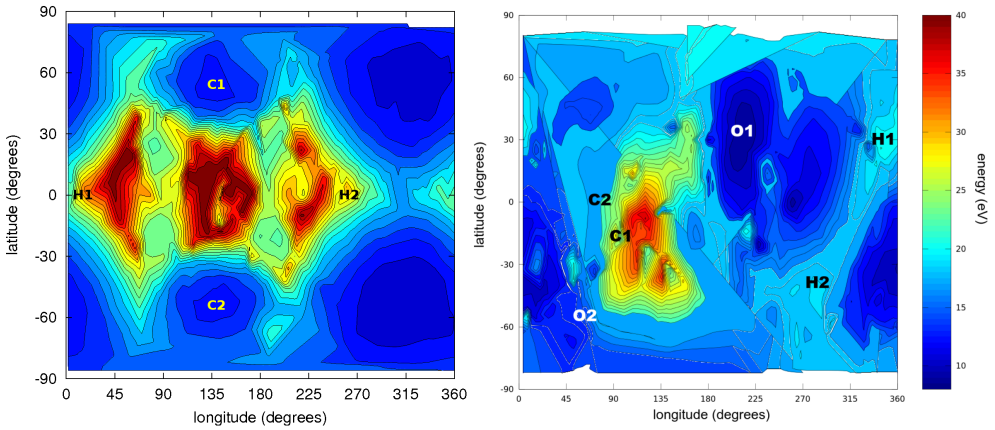


Figure 3: A 2D energy landscape showing the damage threshold energy of a carbon atom in PE chain (left) and in cellulose chain (right), as a function of spherical coordinates, latitude on the $y$-axis and longitude on the $x$-axis.

nar maps, the polar regions in the images are strongly elongated in the horizontal direction. Using these 500 data points as base values, the map grid is filled with interpolated values, of which the final map is composed. The white bands in the top and bottom of the maps are caused by insufficient number of data points occurring in the pole regions due their small area.

In the LHS of Fig. 3, the damage threshold map for carbon atom in PE, we see threshold energy values ranging from 8.8 eV to 40 eV. Creating damage requires most energy (red regions in the map) when the recoil pushes the target carbon atom between its carbon neighbours, or perpendicular to that direction in equatorial zone of the map. Damage is created with the lowest recoil energies when the carbon atom is pushed along the direction of its C-C bonds. In these cases, most of the recoil energy is used for breaking a single C-C bond, instead of dividing it more evenly between two C-C bonds.

The damage threshold map for a carbon target in cellulose chain is shown in the RHS of Fig. 3. The energy range in the map is almost identical to the PE case, the lowest threshold energies are 8.2 eV and the highest 39 eV. Highest energy is needed for damage production when the carbon atom is pushed towards its C1 neighbour and the glucose ring. Damage is created with lowest recoil energies when the recoiling carbon is pushed towards its O1 neighbour. When the recoil causes damage, it typically means that either OH radical or $CH_2OH$ radical is produced, those both occur with equal 40% probability. Free hydrogens are then produced after 20% of the cases.

### *3.2. Recoil event simulations*

The distribution of free radicals and other molecules from 50 and 100 eV single recoil event simulations of HDPE and cellulose is shown in Fig. 4. On the LHS are the results for PE and on the RHS the results for cellulose. In the cellulose simulations we didn't include hydrogen recoils, since the simulation box was shorter in $z$-direction (3.1 nm) than the HDPE box (4.1 nm), and for that reason the recoiling hydrogens had a high tendency to escape the periodic boundaries of the simulation box.

The H recoil events on PE system produce dominantly free H atoms and $H_2$ molecules. With 50 eV recoil energy, H recoils produce almost 3 times more free molecules than C recoils (1.5 vs. 0.58 molecules per recoil event). With 100 eV energy both recoil types produce about the same amount of free molecules (~2.4 molecules per recoil event).

When comparing the PE and cellulose results it is useful to ignore the H recoils and concentrate on the C recoils (red and blue bars in Fig. 4). With 50 eV recoil energy, the number of free molecules produced per recoil event is lower for PE (0.58) than for cellulose (0.85), but with 100 eV recoil energy, the recoil events on PE system produce more free molecules than recoils on cellulose system, 2.4 and 1.4 free molecules per recoil event, respectively.

The most notable difference between the free molecule distributions in Fig. 4 is in the number of H atoms and $H_2$ molecules, in the PE system we have more H atoms than $H_2$ molecules and in the cellulose system almost all hydrogen is in the molecular form. The most probable reason for this is the longer simulation time used in the cellulose simulations — 20 ps vs. 10 ps in

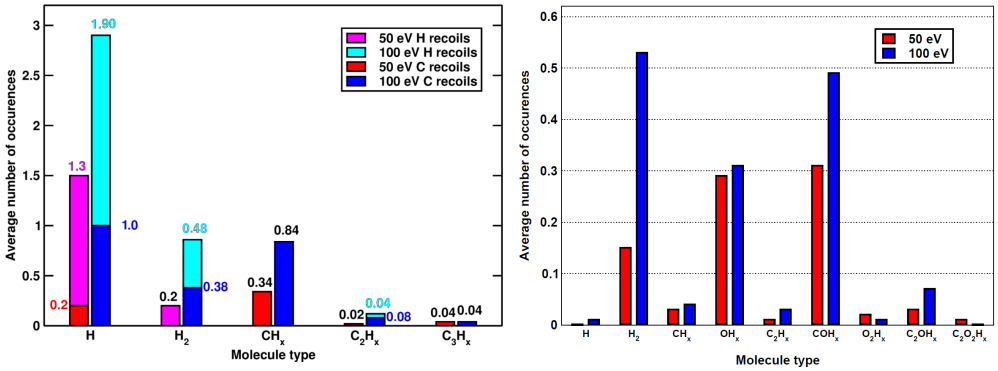


Figure 4: The distribution of free radicals and other molecules produced as a result of 50 and 100 eV recoil events. On the LHS we have the results from HDPE simulations and on the RHS the results from cellulose simulations. Red and magenta bars correspond to 50 eV recoil energy, and blue and cyan bars correspond to 100 eV recoil energy..

PE simulations — which gives single hydrogen atoms more time to combine into $H_2$ molecules.

## 4. Conclusions

The irradiation effects in HDPE and cellulose have been examined using atomistic simulations to better understand the reactions that occur inside the bulk and to compare the irradiation processes in these two widely used materials.

The threshold displacement energy predicted by our damage threshold simulations for carbon in PE, is well in line with the TEM experimental threshold. Both PE and cellulose results also show that the threshold energy for C strongly depends on the direction of the initial recoil with respect to the covalent bonds to the neighbouring carbon and oxygen atoms.

Here we have studied the damage threshold energy for one carbon atom in the cellulose chain. In future work we will continue to determine the threshold energies for all the atoms in the cellulose monomer.

## Acknowledgments

Grants of computer time from CSC – IT Center for Science Ltd in Espoo, Finland, are gratefully acknowledged. J.P. acknowledges funding from Waldemar von Frenckells stiftelse.

[1] Gould, R. F. *Irradiation of Polymers*; American Chemical Society: Washington, D.C., USA, 1967.
[2] Przybytniak, G.; Nowicki, A. *NUKLEONIKA* **2008**, *53(Suppl. 2)*, s67–s72.
[3] Cleland, M. R.; Parks, L. A.; Cheng, S. *Nucl. Instr. Meth. Phys. Res. B* **2003**, *208*, 66–73.
[4] Heiner, A. P.; Sugiyama, J.; Teleman, O. *Carbohydrate Research* **1995**, *273*, 207–223.
[5] Charlesby, A. *Atomic radiation and polymers*; Pergamon Press Inc., 1960.
[6] Chapiro, A. *Radiation Research Supplement* **1964**, *4*, 179–191.
[7] Singh, A. *Radiation Physics and Chemistry* **1999**, *56*, 7556–7570.
[8] Thomas, J. K. *Nucl. Instr. and Meth. B* **2007**, *265*, 1–7.
[9] Perez, C. J. *Radiation Physics and Chemistry* **2010**, *79*, 710–717.
[10] Beardmore, K. *Nuclear Instruments and Methods in Physics Research B* **1995**, *102*, 223–227.
[11] Kovalev, G. V.; Bugaenko, L. T. *High Energy Chemistry* **2003**, *37*, 209–215.
[12] Takács, E.; Wojnáovits, L.; Borsa, J.; Fodváry, C.; Hargittai, P.; Zold, O. *Radiation Physics and Chemistry* **1999**, *55*, 663–666.
[13] Wencka, M.; Wichlacz, K.; Kasprzyk, H.; Lijewski, S.; Hoffmann, S. K. *Cellulose* **2007**, *14*, 183–194.
[14] Desmet, G.; Takács, E.; Wojnárovits, L.; Borsa, J. *Radiation Physics and Chemistry* **2011**, *80*, 1358–1362.
[15] Polvi, J.; Luukkonen, P.; Järvi, T. T.; Kemper, T. W.; Sinnott, S. B.; Nordlund, K. *J. Phys. Chem. B* **2012**, *116*, 13932–13938.
[16] Allen, M. P.; Tildesley, D. J. *Computer Simulation of Liquids*; Oxford University Press: Oxford, England, 1989.
[17] Nordlund, K. 2006; PARCAS computer code. The main principles of the molecular dynamics algorithms are presented in [24, 25]. The adaptive time step and electronic stopping algorithms are the same as in [26].
[18] Stuart, S. J. *Journal Of Chemical Physics* **2000**, *112*, 6472–6486.
[19] Brenner, D. W.; Shenderova, O. A.; Harrison, J. A.; Stewart, S. J.; Ni, B.; Sinnott, S. B. *Journal of Physics: Condensed Matter* **2002**, *14*, 783–802.
[20] Brenner, D. W. *Physical Rewiev B* **1990**, *42*, 9459–9471.
[21] Ni, B.; Lee, K.-H.; Sinnott, S. B. *Journal of Physics: Condensed Matter* **2004**, *16*, 7261–7275.
[22] Kemper, T.; Sinnott, S. B. *Plasma Processes and Polymers* **2012**, *9*, 690–700.
[23] Egerton, R. F.; Li, P.; Malac, M. *Micron* **2004**, *35*, 399–409.
[24] Nordlund, K.; Ghaly, M.; Averback, R. S.; Caturla, M.; Diaz de la Rubia, T.; Tarus, J. *Phys. Rev. B* **1998**, *57*, 7556–7570.
[25] Ghaly, M.; Nordlund, K.; Averback, R. S. *Phil. Mag. A* **1999**, *79*, 795.
[26] Nordlund, K. *Comput. Mater. Sci.* **1995**, *3*, 448.